THE JOURNAL OF BIOLOGICAL CHEMISTRY VOL. 291, NO. 15, pp. 7809–7820, April 8, 2016
Published in the U.S.A.

A G Protein-biased Designer G Protein-coupled Receptor Useful for Studying the Physiological Relevance of $G_{q/11}$-dependent Signaling Pathways*◆

Received for publication, November 4, 2015, and in revised form, January 26, 2016 Published, JBC Papers in Press, February 5, 2016, DOI 10.1074/jbc.M115.702282

Jianxin Hu[‡], Matthew Stern[‡], Luis E. Gimenez[§], Lizzy Wanka[¶], Lu Zhu[‡], Mario Rossi[‡], Jaroslawna Meister[‡], Asuka Inoue[‖], Annette G. Beck-Sickinger[¶], Vsevolod V. Gurevich[§], and Jürgen Wess[‡1]**

*From the [‡]Molecular Signaling Section, Laboratory of Bioorganic Chemistry, NIDDK, National Institutes of Health, Bethesda, Maryland 20892, the [§]Vanderbilt University Medical Center, Nashville, Tennessee 37232, the [¶]Institute of Biochemistry, University of Leipzig, Leipzig 04103, Germany, the [‖]Graduate School of Pharmaceutical Science, Tohoku University, Sendai, Miyagi 980-8578, Japan, and the **Japan Science and Technology Agency, Precursory Research for Embryonic Science and Technology (PRESTO), Kawaguchi, Saitama 332-0012, Japan*

Designer receptors exclusively activated by a designer drug (DREADDs) are clozapine-*N*-oxide-sensitive designer G protein-coupled receptors (GPCRs) that have emerged as powerful novel chemogenetic tools to study the physiological relevance of GPCR signaling pathways in specific cell types or tissues. Like endogenous GPCRs, clozapine-*N*-oxide-activated DREADDs do not only activate heterotrimeric G proteins but can also trigger β-arrestin-dependent (G protein-independent) signaling. To dissect the relative physiological relevance of G protein-mediated *versus* β-arrestin-mediated signaling in different cell types or physiological processes, the availability of G protein- and β-arrestin-biased DREADDs would be highly desirable. In this study, we report the development of a mutationally modified version of a non-biased DREADD derived from the M_3 muscarinic receptor that can activate $G_{q/11}$ with high efficacy but lacks the ability to interact with β-arrestins. We also demonstrate that this novel DREADD is active *in vivo* and that cell type-selective expression of this new designer receptor can provide novel insights into the physiological roles of G protein ($G_{q/11}$)-dependent *versus* β-arrestin-dependent signaling in hepatocytes. Thus, this novel $G_{q/11}$-biased DREADD represents a powerful new tool to study the physiological relevance of $G_{q/11}$-dependent signaling in distinct tissues and cell types, in the absence of β-arrestin-mediated cellular effects. Such studies should guide the development of novel classes of functionally biased ligands that show high efficacy in various pathophysiological conditions but display a reduced incidence of side effects.

During the past few years, designer receptors exclusively activated by a designer drug (DREADDs)[2] have emerged as powerful novel chemogenetic tools to study the physiological relevance of signaling pathways activated by different functional classes of G protein-coupled receptors (GPCRs) (1–3). Structurally, DREADDs represent mutant muscarinic receptors that can be activated by clozapine-*N*-oxide (CNO), an otherwise pharmacologically inert agent, with high potency and efficacy (4, 5). Importantly, these new designer receptors cannot be activated by acetylcholine, the endogenous muscarinic receptor agonist (4, 5).

Recently, DREADDs with different G protein-coupling properties have been expressed in a cell type-specific fashion in mice and other experimental animals, for example by employing classical mouse transgenic approaches or by using viral gene transfer strategies (1–3). CNO treatment of the DREADD-expressing animals then leads to the selective stimulation a distinct GPCR signaling pathways only in DREADD-expressing cells. This approach makes it possible to assess the *in vivo* consequences of activating distinct GPCR signaling pathways in specific cell types. Clearly, such studies are difficult to perform with native GPCRs, which, with virtually no exception, are expressed in multiple tissues and cell types (6).

Agonist binding to GPCRs causes rapid phosphorylation of the activated receptors by GPCR kinases (7, 8). This process promotes the recruitment of members of the arrestin protein family (β-arrestin-1 and -2) to the activated receptors, disrupting receptor/G protein coupling, and promoting GPCR internalization by targeting the receptors to clathrin-coated pits (7, 8). However, during the past 10–15 years, many studies have demonstrated that β-arrestins can also act as signaling molecules in their own right (9–13). This observation is not only of theoretical interest but also of potential clinical relevance (9–11, 14–17).

* This work was supported by the National Institutes of Health Intramural Research Program, NIDDK, United States Department of Health and Human Services (to J. H., M. S., L. Z., M. R., J. M., and J. W.), Deutsche Forschungsgemeinschaft Grant DCRC1052-A3 (to L. W.), National Institutes of Health RO1 Grants GM077561 and GM109955 (to V. V. G.), and PRESTO, Japan Science and Technology Agency (to A. I.). The authors declare that they have no conflicts of interest with the contents of this article. The content is solely the responsibility of the authors and does not necessarily represent the official views of the National Institutes of Health.

◆ This article was selected as a Paper of the Week.

[1] To whom correspondence should be addressed: Molecular Signaling Section, Lab. of Bioorganic Chemistry, NIH-NIDDK, Bldg. 8A, Room B1A-05, 8 Center Drive MSC 0810, Bethesda, MD 20892-0810. Tel.: 301-402-3589; Fax: 301-480-3447; E-mail: jwess@helix.nih.gov.

[2] The abbreviations used are: DREADD, designer receptors exclusively activated by a designer drug; GPCR, G protein-coupled receptor; CNO, clozapine-*N*-oxide; BRET, bioluminescence resonance energy transfer; NMS, *N*-methylscopolamine; AAV, adeno-virus-associated virus; HGP, hepatic glucose production; eGFP, enhanced GFP; TBG, thyroxine-binding globulin; M3R, M_3 muscarinic receptor; M3Dq, M3R-based G_q DREADD; EYFP, enhanced YFP.

Consistent with the GPCR-like properties of DREADDs, two recent studies have demonstrated that the M_3 muscarinic receptor (M3R)-based G_q DREADD (M3Dq) does not only activate G proteins of the G_q family but can also interact with β-arrestin-1 and -2 and trigger β-arrestin-dependent downstream signaling (18, 19). It is likely that other DREADDs are also endowed with the ability to couple to both G protein- and β-arrestin-dependent signaling pathways.

These new findings suggest that the physiological outcome of activating a specific GPCR (or DREADD) in a particular tissue or cell type represents an integrated response caused by the activation of both G protein- and β-arrestin-dependent signaling pathways. To gain insight into the physiological relevance of these two distinct GPCR signaling branches, it is important to assess the relative contribution of G protein- and β-arrestin-dependent signaling to a particular tissue response. To shed light on this issue, we recently generated an M3R-based, β-arrestin-biased DREADD (18) (*M3D-arr* in Fig. 1). In this study, we describe the generation of a novel $G_{q/11}$-biased, M3R-derived DREADD that lacks the ability to interact with β-arrestins (*M3D-Gq* in Fig. 1). We also demonstrate that this novel DREADD is active *in vivo* and that cell type-selective expression of the new designer receptor can lead to novel insights into the physiological roles of G protein-dependent *versus* β-arrestin-dependent signaling (in hepatocytes). This novel $G_{q/11}$-biased DREADD represents a powerful new tool to study the physiological relevance of $G_{q/11}$-dependent signal cascades in distinct tissues and cell types, in the absence of β-arrestin-mediated cellular effects.

These new findings suggest that the physiological outcome of activating a specific GPCR or DREADD in a particular tissue or cell type represents an integrated response caused by the activation of both G protein- and β-arrestin-dependent signaling pathways. To gain insight into the physiological relevance of these two distinct GPCR signaling branches, it is important to assess the relative contribution of G protein- and β-arrestin-dependent signaling to specific tissue response(s). Importantly, such information could be exploited for developing novel classes of clinically useful drugs, including G protein or β-arrestin-biased agonists (9–11, 14–16).

Experimental Procedures

Drugs—Acetylcholine chloride, carbamylcholine chloride (carbachol), and atropine sulfate were obtained from Sigma. *N*-[^{3}H]Methylscopolamine ([^{3}H]NMS; 85.4 Ci/mmol) was purchased from PerkinElmer Life Sciences. Clozapine-*N*-oxide (CNO) was obtained from the National Institutes of Health as part of the Rapid Access to Investigative Drug Program funded by the NINDS.

Generation of a New Designer GPCR (DREADD)—To generate an M3R-based DREADD that is able to couple to G_q-type G proteins but lacks the ability to recruit β-arrestins, we introduced the following mutations into the M3D DREADD described by Guettier *et al.* (5). We removed the central portion of the third intracellular (i3) loop (Ala-274–Lys-469) and introduced four point mutations (C542A, C546S, C560S, and C562S) by using the QuikChange™ site-directed mutagenesis kit (Stratagene, La Jolla, CA), according to the manufacturer's instructions. Amino acid numbers refer to the rat M3R sequence. For the sake of simplicity, we refer to this newly generated DREADD simply as "M3D-Gq." The M3D-Gq coding sequence was inserted into the pcDNA3.1(−) vector (Invitrogen) using standard cloning techniques. The entire M3D-Gq coding sequence was sequenced to exclude the presence of any unwanted mutations. All DREADDs used in this study carried an N-terminal HA epitope tag (5, 18) and were cloned into the pcDNA3.1(−) vector.

Transient Expression of DREADDs in Cultured Cells—DREADD/receptor constructs were transiently expressed in COS-7 or HEK293 cells using Lipofectamine 2000 according to the manufacturer's protocol (Thermo Fisher Scientific; for more details, see Ref. 20). Transfected COS-7 cells were incubated with 1 μM atropine for the last 24 h of culture, to obtain higher receptor densities. About 48 h after transfections, cells were harvested and used for radioligand binding or functional assays.

Radioligand Binding Studies—Radioligand binding studies were performed with membrane preparations obtained from transfected COS-7 cells as described previously (20). In brief, binding reactions containing ~10 μg of membrane protein per tube were carried out for 2 h at 22 °C in 0.5 ml of binding buffer containing 25 mM sodium phosphate and 5 mM $MgCl_2$ (pH 7.4). In saturation binding assays, we employed six different [^{3}H]NMS concentrations (1.5–50 nM). In competition binding assays, we used a fixed concentration of [^{3}H]NMS (5 nM) in the presence of 10 different concentrations of CNO or acetylcholine. Nonspecific binding was defined as binding observed in the presence of 10 μM atropine. Binding reactions were terminated by rapid filtration over GF/C glass fiber filters (Brandel, Gaithersburg, MD), followed by three washes (~4 ml per wash) with ice-cold distilled water. The amount of radioactivity that remained bound to the filters was determined by liquid scintillation spectrometry. Binding data were analyzed by using the nonlinear curve-fitting program Prism 6.04 (GraphPad Software, San Diego).

Calcium Mobilization Assay—COS-7, WT HEK293, or $G\alpha_{q/11}$-deficient HEK293 cells transiently expressing DREADDs with different coupling properties were resuspended in DMEM supplemented with 10% fetal bovine serum and grown in collagen-coated 96-well plates (black-walled, clear bottom; Thermo Scientific). Cells were plated at a density of 2.5×10^4 cells per well. About 48 h after transfection, CNO-induced changes in intracellular calcium levels ($[Ca^{2+}]_i$) were measured via FLIPR (Molecular Devices, Sunnyvale, CA), as described previously (21). After a washing step (200 μl of Hanks' balanced salt solution containing 20 mM HEPES (pH 7.4) per well), 30 μl of loading dye (FLIPR calcium 3 assay kit containing the proprietary calcium 3 fluorophore; Molecular Devices), supplemented with 2.5 mM probenecid to increase dye retention, was added to each well, followed by a 45-min incubation at 37 °C. Cells were then incubated with increasing concentrations of CNO, and changes in cell fluorescence were measured at 22 °C via FLIPR (FLIPR TETRA; excitation wavelength, 470–495 nm; emission wavelength, 515–575 nm). For each CNO dose, we measured increases in intracellular calcium levels as peak fluorescence activity minus basal fluorescence activity prior to the addition of CNO. Cells expressing the wild-type (WT) M3R were pro-

cessed in the same fashion as DREADD-expressing cells, except that carbachol and acetylcholine were used as agonists. Agonist E_{max} and EC_{50} values were obtained by analyzing concentration-response curves via GraphPad Prism 6.04 (GraphPad Software, San Diego). All assays were carried out in quadruplicate.

Using the same experimental setup, we also carried out FLIPR assays with primary hepatocytes isolated from mice injected with recombinant adeno-associated viruses (AAVs; see below) coding for the various DREADDs used in this study. Primary hepatocytes were plated at a density of 1.2×10^4 cells per well in 96-well plates. All experimental conditions remained the same as described in the previous paragraph, except that hepatocytes were incubated at 37 °C for 75 min after the addition of the loading dye (100 μl).

Western Blotting Studies—Immunoblotting experiments were carried out using published protocols (20, 21). In brief, samples containing 20 μg of solubilized membrane protein were incubated with Laemmli loading buffer (30 min at 37 °C) under reducing conditions, loaded onto 10% Tris-glycine polyacrylamide gels (Invitrogen), and run at 135 V in the presence of 0.1% SDS. Immunoblots were probed with a rabbit monoclonal anti-HA antibody (catalog no. C29F4, Cell Signaling, Boston, MA) or a mouse monoclonal anti-FLAG antibody (catalog no. A00187, GenScript, Piscataway Township, NJ). Immunoreactive proteins were visualized by using SuperSignal West Pico Chemiluminescent Substrate (Pierce).

Co-immunoprecipitation—Experiments were carried out as described (21). COS-7 cells were co-transfected with DREADDs containing an N-terminal HA tag and a β-arrestin-1 construct carrying a C-terminal FLAG tag (ID 14687, Addgene, Cambridge, MA). About 48 h after transfection, cells were treated with 10 μM CNO for 10 min at 37 °C and then solubilized in lysis buffer containing 1% digitonin, 25 mM sodium phosphate, 5 mM $MgCl_2$ (pH 7.4), and complete protease and PhosSTOP phosphatase inhibitor cocktails (Roche Applied Science). Solubilized membrane proteins (~600 μg per tube) were incubated for 1 h at 4 °C with an anti-FLAG monoclonal antibody (catalog no. A00187, GenScript, Piscataway, NJ). After this step, 30 μl of protein A/G-agarose (Santa Cruz Biotechnology, Dallas, TX) were added, followed by an additional incubation period of 1 h at 4 °C. Bound immunoreactive proteins were eluted, and immunoblotting studies were performed using the rabbit monoclonal anti-HA antibody (see previous paragraph), as described in detail previously (21).

BRET Studies—The ability of the various DREADDs to recruit β-arrestin-1 or -2 was assessed in BRET assays. The construction and use of DREADD-*Renilla* luciferase (Luc) variant 8 fusion proteins have been described previously (18). In an analogous fashion, we generated M3D-Luc and M3D-Gq-Luc constructs (vector: pcDNA3.1(−)). The generation of Venus-tagged β-arrestin-1 and -2 constructs (V-β-arrestin-1 or -2; vector, pcDNA3.1(−)) suitable for BRET studies has also been reported previously (18, 22–24). COS-7 cells growing in 60-mm cell culture dishes were transiently co-transfected with a fixed amount (0.1–0.2 μg) of DREADD-Luc construct and varying amounts of V-β-arrestin-1 or -2 DNA (0–12 μg) using Lipofectamine 2000 (Thermo Fisher Scientific). Cells were transferred to white 96-well plates (5×10^4 cells/well) 1 day after transfection. Forty eight hours after transfection, cells were incubated for 20 min with 5 μM coelenterazine-*h* (Nanolight Technology Pinetop, AZ) and 20 μM CNO (or vehicle), followed by the measurement of luminescence at 460 and 535 nm. Net BRET (the difference between BRET ratios with and without agonist) determined after CNO treatment was plotted as a function of the acceptor (V-β-arrestin) fluorescence over donor (DREADD-Luc) luminescence ratio. Acceptor fluorescence was determined using cells growing in black 96-well plates (excitation/emission, 485/535 nm). CNO (0.5 nM to 400 μM) concentration-response curves were obtained by following a similar protocol. COS-7 cells seeded into 100-mm dishes were co-transfected with 0.1–0.2 μg of a particular DREADD-Luc plasmid and 20 μg of V-β-arrestin-1 or -2 DNA. The resulting curves were fit by non-linear regression to a one-site hyperbola (BRET saturation curves with increasing amounts of V-β-arrestin DNA) or a three-parameter sigmoidal curve (CNO concentration-response curves) using GraphPad Prism 6.04 (GraphPad Software, San Diego).

Live-cell Imaging of DREADD Internalization Using Fluorescence Microscopy—HEK293 cells were plated onto sterile 8-well μ-slides (Ibidi GmbH, Martinsried/Munich, Germany), grown to 70% confluence, and then transfected using Lipofectamine 2000 with plasmids encoding DREADDs carrying a C-terminal EYFP tag (0.9 μg DNA per construct). The DREADD-EYFP constructs were generated using standard cloning techniques (vector, pcDNA3). Live-cell imaging was performed 24 h after transfection using a Zeiss Axio Observer microscope with an Apo Tome Imaging System equipped with a heating insert P-Lab-Tec S1 unit. Fluorescence images were taken from living cells at 37 °C on a heated microscope stage using AxioVision Rel. 4.6 software. Cells were starved for 30 min in serum-free Opti-MEM® medium (Thermo Fisher Scientific), and cell nuclei were stained with Hoechst 33342 (5 μg/μl) for 10 min. To study DREADD internalization, cells were incubated with carbachol or CNO (100 μM each) for 45 min. Images were acquired before and after agonist treatment.

Generation of DREADD-encoding Recombinant AAVs—The DREADD-coding sequences containing an N-terminal HA tag were subcloned into the AAV-TBG-MCS plasmid (a kind gift from Dr. Morris Birnbaum, University of Pennsylvania, Philadelphia) (25). *Escherichia coli* SURE cells (Agilent Technologies, Santa Clara, CA), which are deficient in *E. coli* genes involved in the rearrangement and deletion of DNA, were used as host cells to reduce the likelihood of recombination events due to the presence of the ITR sequences in the AAV-TBG-MCS plasmid. This strategy yielded the following three recombinant viral constructs: AAV-TBG-M3D, AAV-TBG-M3D-arr, and AAV-TBG-M3D-Gq. AAV viral particles were generated by the University of Pennsylvania Vector Core. The AAV-TBG-eGFP control virus (catalog no. AV-8-PV0146) was obtained through the same source.

Mouse Maintenance and Diet—C57BL/6NTac (Taconic, Germantown, NY) were housed in a specific pathogen-free barrier facility maintained on a 12-h light, 12-h dark cycle (light period from 6:00 a.m. to 6:00 p.m.). Mice were fed *ad libitum* with standard mouse chow (4% (w/w) fat content; Zeigler,

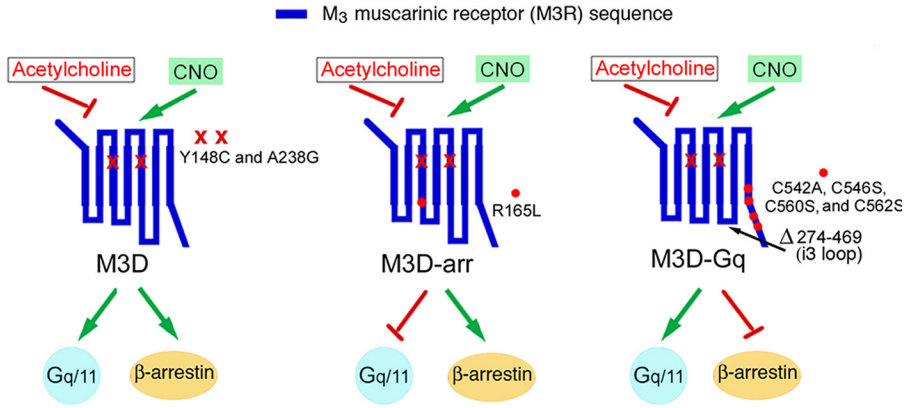


FIGURE 1. **Structure, nomenclature, and functional profile of DREADDs used in this study.** The M3D DREADD shown in the *left panel* (*M3D*; full name according to Ref. 4) is M3Dq) can couple to both G_q-type G proteins and recruit β-arrestins (4, 5, 18, 19). The M3D-arr DREADD (*center panel*) represents a β-arrestin-biased version of M3D that contains the R165L point mutation (18). The *right panel* depicts the $G_{q/11}$-biased DREADD (*M3D-Gq*) that we developed and characterized in this study. When activated by CNO, the M3D-Gq designer receptor efficiently activates $G_{q/11}$ but fails to recruit β-arrestins (see text for details). The M3D-Gq construct lacks the central portion of the third intracellular (i3) loop (Ala-274–Lys-469) and contains four additional point mutations: C542A, C546S, C560S, and C562S. Amino acid numbers refer to the rat M3R sequence. *M3R*, M_3 muscarinic receptor.

Gardners, PA). All animal studies were approved by the Animal Care and Use Committee of the NIDDK, National Institutes of Health (Bethesda, MD).

Selective Expression of DREADDs in Mouse Liver/Hepatocytes—AAVs (AAV-TBG-M3D, AAV-TBG-M3D-arr, AAV-TBG-M3D-Gq, and AAV-TBG-eGFP) were injected into the tail vein of WT C57BL/6NTac mice (8-week-old males) by using an insulin syringe (0.5-ml; needle, 28-gauge, ½-inch long, 0.36 × 13 mm) loaded with 100 μl of diluted AAV solution (10^{11} AAV genomic copies per 100 μl). Each mouse received 10^{11} genomic copies regardless of body weight. Two to 3 weeks after AAV injections, the liver-specific expression of the various DREADDs was determined via Western blotting. The number of DREADD-binding sites in the liver was determined in [^{3}H]NMS binding studies using liver membrane homogenates. [^{3}H]NMS binding studies were carried out in the same fashion as described above for transfected COS-7 cells.

DREADD-mediated Increases in Blood Glucose Levels—Two weeks after AAV treatment (see previous paragraph), mice were injected with CNO (10 mg/kg intraperitoneally). Blood samples were taken from the mouse tail just prior to injection (time "0") and 15, 30, 60, and 90 min post-injection. Blood glucose levels were measured with an automated blood glucometer (Contour, Bayer, Whippany, NJ).

DREADD-mediated Increases in Hepatic Glucose Production Studied with Primary Hepatocytes—Two weeks after AAV treatment of WT C57BL/6NTac mice, primary hepatocytes were harvested as described earlier (26). Hepatocytes were first cultured in 12-well plates (phenol red-free DMEM containing 10% FBS and 1 g/liter glucose) for ~4 h at 37 °C. The medium was then replaced with glucose- and phenol red-free DMEM supplemented with gluconeogenic substrates (20 mM sodium lactate and 2 mM sodium pyruvate), followed by a 16-h incubation at 37 °C. Subsequently, hepatocytes were incubated in the same medium in the presence or absence of glucagon (100 nM; positive control) or CNO (10 μM) for 4 h at 37 °C. After this time, the culture medium was collected for the measurement of glucose levels.

Knockdown of $G\alpha_{q/11}$ Expression in Primary Mouse Hepatocytes—M3D-Gq-expressing hepatocytes were isolated from AAV-injected mice and plated in 6-well plates (5×10^5 cells per well) in DMEM containing 10% FBS. To knock down $G\alpha_{q/11}$ expression, hepatocytes were transfected with $G\alpha_q$ and $G\alpha_{11}$ siRNAs (On Target plus siRNA SMARTpools, GE Dharmacon, Lafayette, CO) or scrambled control siRNA using Lipofectamine RNAiMAX transfection reagent (Thermo Fisher Scientific). About 24 h later, hepatocytes were processed for glucose output measurements as described in the previous paragraph. At the end of the experiment, cells were harvested for the isolation of total RNA. $G\alpha_q$ and $G\alpha_{11}$ transcript levels were determined by quantitative RT-PCR. The following primer pairs were used: $G\alpha_q$, 5′-TTGGTTCGAGAGGTTGATGTG-3′ and 5′-CGTCGTCTGTCGTAGCACTC-3′; $G\alpha_{11}$, 5′-CAACGCGGAGATCGAGAAACA-3′ and 5′-GCCTGCATGGCGGTAAAGAT-3′.

Receptor Internalization Studies with M3D-arr-Expressing Hepatocytes—To confirm that the M3D-arr receptor remained functional *in vivo*, we carried out internalization assays using primary hepatocytes expressing the M3D-arr construct. Hepatocytes growing in collagen-coated 6-well plates were incubated with CNO (10 μM) for 60 min at 37 °C in DMEM containing 300 mM HEPES (incubation volume: 2 ml). After this step, cells were incubated for 2 h at 4 °C in the same buffer with 10 nM [^{3}H]NMS, a membrane-impermeable radioligand, as described in detail previously (27). Nonspecific binding was determined in the presence of 10 μM atropine. Assays were carried out in duplicate.

Statistics—Data are expressed as means ± S.E. for the indicated number of observations. For comparisons between two groups, the unpaired Student's *t* test (two-tailed) was used. A p value of <0.05 was considered statistically significant.

Results

Generation of a $G_{q/11}$-Biased DREADD—Using the non-biased M3Dq DREADD (4, 5) as a template, we recently generated an arrestin-biased version of this DREADD (18). For sim-

plicity, we will refer to the non-biased DREADD as "M3D" and to the arrestin-biased DREADD as "M3D-arr," respectively (Fig. 1). To generate an M3D-derived DREADD that retains the ability to activate G proteins of the G_q family but is unable to recruit β-arrestins, we screened a series of mutationally modified M3D constructs in transfected COS-7 cells.

The agonist-activated M3R is phosphorylated on multiple serine residues within the third intracellular (i3) loop (28, 29), and simultaneous replacement of most of these residues with alanine causes a pronounced reduction in both agonist-dependent M3R phosphorylation and β-arrestin recruitment (30). However, deletion of most of the i3 loop of the M3R (deletion of amino acids Ala-274–Lys-469; rat M3R sequence) does not interfere with the ability of the WT M3R to activate G_q-type G proteins (31, 32). On the basis of these observations, we introduced the Ala-274–Lys-469 deletion into the M3D construct. However, pilot BRET experiments showed that this structural modification was not sufficient to completely prevent M3D-mediated β-arrestin recruitment, in agreement with data presented by Kong *et al.* (30).

Various lines of evidence (33–36), including recent high resolution structural information of GPCR-arrestin complexes (37, 38), indicate that residues within the C-terminal portion of transmembrane helix 7 and the adjacent helix 8 play important roles in mediating the conformational changes required for productive GPCR/arrestin interactions. Prompted by these findings, we introduced a series of point mutations into the cytoplasmic end of transmembrane helix 7 and helix 8 of the M3D construct lacking Ala-274–Lys-469. This approach eventually yielded a mutationally modified version of M3D that retained the ability to activate G_q-type G proteins in an M3D-like fashion, but it was no longer able to recruit β-arrestins. For the sake of simplicity, we refer to this $G_{q/11}$-biased DREADD as M3D-Gq (Fig. 1). Besides the Ala-274–Lys-469 deletion, this new DREADD contains four additional point mutations, two in the C-terminal portion of transmembrane helix 7 (C542A and C546S) and two at the end of helix 8 (C560S and C562S) (Fig. 1). Below we will describe the pharmacological and functional properties of this novel DREADD. In addition, we demonstrate that the M3D-Gq DREADD represents a highly useful tool for distinguishing between G protein-mediated *versus* β-arrestin-mediated signaling pathways *in vivo*.

Ligand Binding Properties of M3D-Gq—To determine the ligand properties of M3D-Gq, we performed [^{3}H]NMS saturation and competition binding studies, using membranes prepared from transfected COS-7 cells. WT M3R-containing membranes were included for control purposes in all experiments. [^{3}H]NMS saturation binding studies showed that M3D-Gq was expressed at similarly high levels as the M3D parent DREADD and that M3D-Gq, similar to M3D, was able to bind CNO with high affinity (K_i ~1 μM; Table 1). In contrast, both DREADDs failed to bind acetylcholine, the physiological muscarinic receptor agonist (highest concentration tested: 0.3 mM; Table 1).

M3D-Gq Retains the Ability to Couple to $G_{q/11}$—To investigate whether M3D-Gq retained the ability to activate G proteins of the G_q family, we initially studied CNO-induced increases in intracellular calcium levels $[Ca^{2+}]_i$ in DREADD-expressing COS-7 cells. FLIPR studies showed that CNO treatment of M3D-Gq-expressing cells caused pronounced concentration-dependent increases in $[Ca^{2+}]_i$, in a fashion similar to that observed with cells expressing the non-biased M3D DREADD (Table 2 and Fig. 2*A*), indicating that M3D-Gq retains the ability to efficiently couple to $G_{q/11}$. In contrast, exposure of M3D-Gq- or M3D-expressing cells to acetylcholine or carbachol did not lead to significant increases in $[Ca^{2+}]_i$ (Table 2).

We obtained very similar results when we carried out FLIPR studies with transfected WT HEK293 cells (Fig. 2*B*). Strikingly, the M3D-Gq- and M3D-mediated calcium responses were completely abolished in HEK293 cells lacking both $G\alpha_q$ and $G\alpha_{11}$ ($G\alpha_{q/11}$ KO HEK293 cells (39)). Co-expression of $G\alpha_q$ with M3D-Gq in $G\alpha_{q/11}$ KO HEK293 cells rescued the CNO/M3D-Gq-mediated increase in $[Ca^{2+}]_i$ (Fig. 2*C*). These data clearly indicate that the CNO/M3D-Gq-triggered elevation in $[Ca^{2+}]_i$ is mediated by G_q-type G proteins.

DREADD/Arrestin Interactions Studied Via BRET—We next used BRET technology to examine the ability of M3D-Gq to

TABLE 1

Ligand binding properties of receptors/DREADDs expressed in COS-7 cells

The WT human M3R (hM3R) and the indicated DREADDs were transiently expressed in COS-7 cells. [^{3}H]NMS saturation and [^{3}H]NMS/agonist (acetylcholine or CNO) competition binding experiments were performed using membrane homogenates as described under "Experimental Procedures." Data are presented as means ± S.E. of 3–7 independent experiments, each performed in duplicate.

Receptor	[^{3}H]NMS		Acetylcholine, K_i	CNO, K_i
	K_D	B_{max}		
	nM	*pmol/mg of protein*	*μM*	*μM*
WT hM3	0.53 ± 0.16	5.51 ± 0.81	27.3 ± 14.9	ND[a]
M3D	8.5 ± 2.1	3.52 ± 0.63	NB[b]	0.89 ± 0.25
M3D-Gq	10.4 ± 1.3	3.45 ± 0.67	NB[b]	1.12 ± 0.54

[a] ND means not determined (4, 5).
[b] NB means no significant binding up to 0.3 mM.

TABLE 2

M3R/DREADD-mediated increases in $[Ca^{2+}]_i$ in transfected COS-7 cells

The WT human M3R (hM3R) and the indicated DREADDs were transiently expressed in COS-7 cells. Agonist-induced increases in $[Ca^{2+}]_i$ were measured using FLIPR, as described under "Experimental Procedures." The carbachol EC_{50} value obtained with WT M3R-expressing cells is in good agreement with published results (20, 50). Data are presented as means ± S.E. of at least three independent experiments, each performed in quadruplicate.

Receptor	Carbachol-induced Ca^{2+} mobilization		Acetylcholine-induced Ca^{2+} mobilization		CNO-induced Ca^{2+} mobilization	
	EC_{50}	E_{max}	EC_{50}	E_{max}	EC_{50}	E_{max}
	nM	*-fold over basal*	*nM*	*-fold over basal*	*nM*	*-fold over basal*
WT hM3R	31.9 ± 8.9	3.9 ± 0.2	16.7 ± 9.7	3.5 ± 0.5	ND[a]	
M3D	NR[b]		NR[b]		63.3 ± 12.3	12.9 ± 3.4
M3D-Gq	NR[b]		NR[b]		68. 9 ± 2.8	13.2 ± 2.6

[a] ND means not determined (4, 5).
[b] NR means no significant response in the investigated concentration range (up to 0.5 mM).

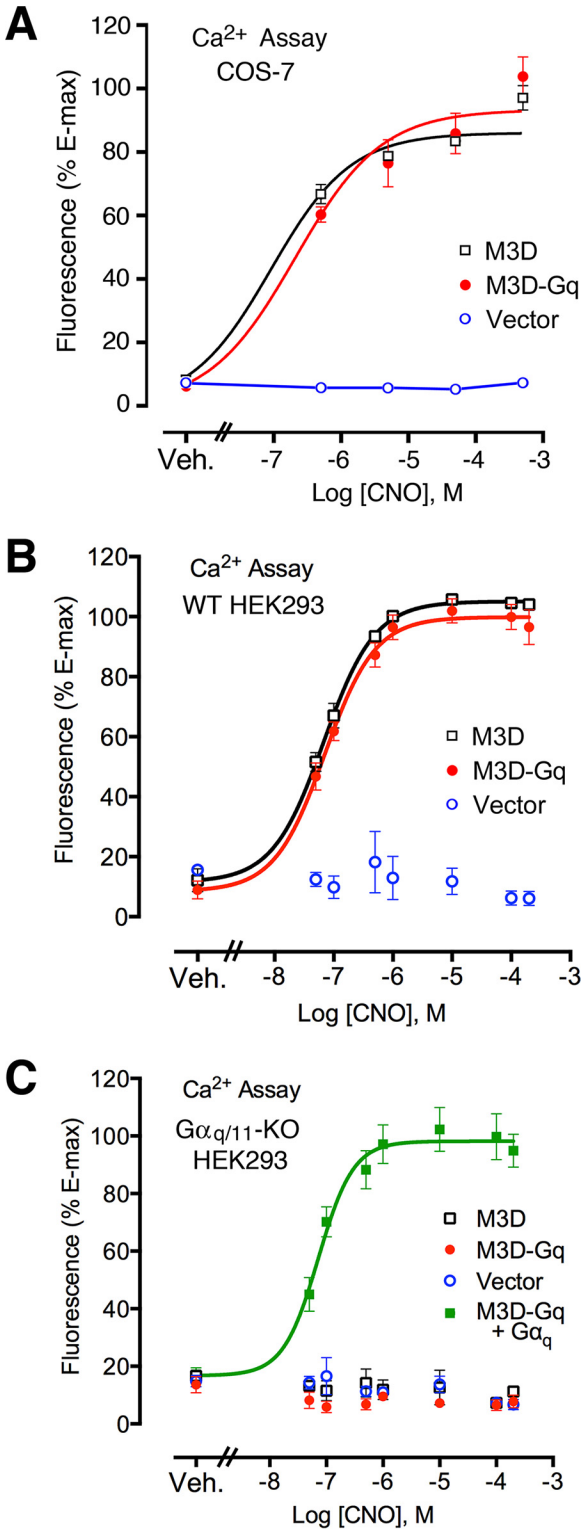


FIGURE 2. **CNO treatment of M3D-Gq-expressing cultured cells leads to a $G_{q/11}$-mediated increase in $[Ca^{2+}]_i$.** *A–C*, COS-7 (*A*), WT HEK293 (*B*), or $G\alpha_{q/11}$-deficient HEK293 (*C*) cells were transfected with the indicated constructs. CNO-induced increases in $[Ca^{2+}]_i$ were determined using FLIPR, as described under "Experimental Procedures." The curves shown in *A* are from a representative experiment, carried out in quadruplicate. Two additional experiments gave similar results (mean CNO EC_{50} and E_{max} values are given in Table 2). The data shown in *B* and *C* represent means ± S.E. from three independent experiments, each performed at least in triplicate. $G\alpha_q$, human $G\alpha_q$ inserted into the pcDNA3.1 expression plasmid. *Veh*, vehicle.

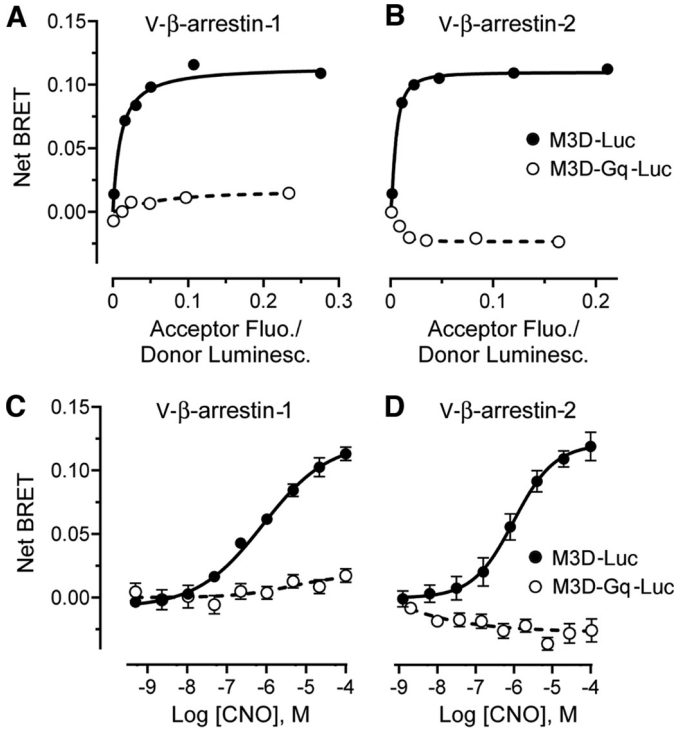


FIGURE 3. **BRET analysis of DREADD/β-arrestin interactions.** *A–D*, COS-7 cells were co-transfected with luciferase (*Luc*)-tagged versions of M3D or M3D-Gq (luminescence donor) and β-arrestin-1 or -2 constructs carrying an N-terminal Venus fluorescence acceptor (*V*). BRET measurements were performed to monitor CNO-dependent DREADD/β-arrestin interactions as described under "Experimental Procedures." *A* and *B*, BRET measurements were carried out in the presence of a fixed concentration of CNO (20 μM). BRET signals are expressed as net BRET values obtained by subtracting the net BRET ratio measured in the absence of CNO from the corresponding value obtained in its presence. *C* and *D*, CNO concentration-response curves for CNO-dependent recruitment of β-arrestin-1 (*C*) or -2 (*D*) by the two DREADDs. In contrast to M3D, the M3D-Gq DREADD fails to recruit β-arrestins in these assays. Data are given as means ± S.E. from a representative experiment carried out in quadruplicate. Two additional experiments gave similar results. The CNO pEC_{50} values for M3D-mediated β-arrestin recruitment were as follows: β-arrestin-1, 6.52 ± 0.23; β-arrestin-2, 6.08 ± 0.08 (n = 3).

recruit β-arrestins in a CNO-dependent fashion. Following established protocols (22–24), we co-transfected COS-7 cells with DREADD constructs (M3D or M3D-Gq) containing a C-terminal *Renilla* luciferase 8 sequence (M3D-Luc or M3D-Gq-Luc, respectively; BRET donor) and β-arrestin-1 or -2 constructs carrying an N-terminal Venus tag (V-β-arrestin-1 or V-β-arrestin-2, respectively; BRET acceptor).

Initially, we transfected cells with a fixed amount of DREADD-Luc construct and varied the amount of co-transfected V-β-arrestin plasmids. The following day, we measured luminescence at 460 and 535 nm after incubation of cells with coelenterazine-*h* and 20 μM CNO (or vehicle for unstimulated cells). In the case of M3D-Luc-expressing cells, this approach led to saturable net BRET curves in the presence of increasing amounts of V-β-arrestin-1 or -2 (Fig. 3, *A* and *B*). In contrast, no significant increases in net BRET were observed with M3D-Gq-Luc-expressing cells under the same experimental conditions (Fig. 3, *A* and *B*).

In another set of BRET experiments, we co-transfected COS-7 cells with fixed amounts of DREADD-Luc and V-β-arrestin-1 or -2 DNA. The next day, we carried out BRET mea-

surements in the presence of increasing concentrations of CNO as described in the previous paragraph. Consistent with published data (18, 19), CNO treatment of cells co-expressing M3D-Luc and V-β-arrestin-1 or -2 led to concentration-dependent net BRET signals, indicative of CNO-dependent β-arrestin recruitment (Fig. 3, *C* and *D*). In contrast, no significant increases in net BRET were observed with M3D-Gq-Luc-expressing cells under the same experimental conditions (Fig. 3, *C* and *D*). This latter observation strongly suggests that the M3D-Gq DREADD lacks the ability to recruit β-arrestins in an agonist (CNO)-dependent fashion. On the contrary, using a similar experimental strategy, we recently showed the M3D-arr-Luc construct can interact with both V-β-arrestin-1 and -2 (18).

Detection of DREADD/Arrestin Interactions Via Co-immunoprecipitation—To confirm the inability of M3D-Gq to recruit β-arrestins with a different experimental approach, we carried out co-immunoprecipitation studies. Lysates from COS-7 cells co-transfected with HA-tagged versions of the different DREADD constructs and FLAG-tagged β-arrestin-1 were treated with an anti-FLAG monoclonal antibody to immunoprecipitate β-arrestin-1, followed by immunoblotting studies using an anti-HA antibody to detect co-immunoprecipitated DREADDs.

The anti-HA antibody detected a specific ~120-kDa immunoreactive species when cells had been co-transfected with HA-M3D or HA-M3D-arr and the β-arrestin-1 construct (Fig. 4*A*, *right panel*). The intensity of this band was greatly increased after exposure of cells to CNO (10 μM), indicating that complex formation between M3D or M3D-arr and β-arrestin-1 was strongly enhanced by DREADD activation. In striking contrast, no specific immunoreactive band was observed after co-transfection of cells with HA-M3D-Gq and the β-arrestin-1 construct (Fig. 4*A*, *right panel*) or with cell lysates from cells expressing M3D, M3D-Gq, or β-arrestin-1 alone (Fig. 4*B*, *right panel*).

Live-cell Imaging of DREADD Internalization—One of the classical roles of β-arrestins is to mediate the internalization of activated GPCRs (8, 40). To investigate DREADD internalization, we transiently expressed M3D, M3D-Gq, and M3D-arr in HEK293 cells. For comparison, we also studied cells transfected with the WT M3R. All receptor constructs used in these studies carried a C-terminal EYFP tag.

We then used fluorescence microscopy to measure agonist-dependent receptor/DREADD internalization in live cells. Prior to agonist simulation, nearly all receptors/DREADDs were expressed on the cell surface (Fig. 5). Following agonist treatment of WT M3R-, M3D-, and M3D-arr-expressing cells, a significant receptor population was internalized (Fig. 5). However, this effect was not observed after agonist (CNO) stimulation of M3D-Gq-expressing cells (Fig. 5). These findings are in good agreement with the notion that the M3D-Gq DREADD is unable to recruit β-arrestins.

Expression of DREADDs in Hepatocytes in Vivo Using Recombinant AAVs—To study whether the newly generated M3D-Gq DREADD was also active *in vivo*, we used a viral strategy to selectively express M3D-Gq in hepatocytes of WT C57BL/6NTac mice. Specifically, we generated a recombinant AAV coding for M3D-Gq under the control of the hepatocyte-specific TBG promoter (AAV-TBG-M3D-Gq). Using the same strategy, we also generated AAVs coding for M3D, M3D-arr, and eGFP (for control purposes) (note that all DREADDs contained an N-terminal HA tag). All AAVs (AAV-TBG-M3D, AAV-TBG-M3D-arr, AAV-TBG-M3D-Gq, and AAV-TBG-eGFP) were injected into the tail vein of WT C57BL/6NTac mice.

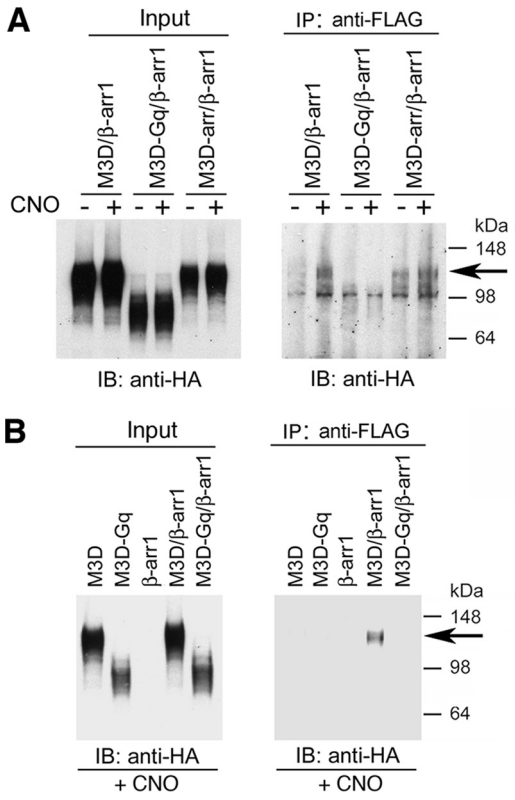


FIGURE 4. **Use of co-immunoprecipitation to study DREADD/β-arrestin interactions.** *A,* COS-7 cells were co-transfected with the indicated DREADDs carrying N-terminal HA tags and a FLAG-tagged version of β-arrestin-1 (*β-αrr1*). About 48 h after transfection, cells were incubated for 20 min either without (−) or with (+) CNO (10 μM). Subsequently, cell extracts were immunoprecipitated with a mouse monoclonal anti-FLAG antibody, and the precipitated proteins were subjected to Western blotting analysis using a rabbit monoclonal anti-HA antibody. For comparison, immunoblots (*IB*) of cell lysates prior to the immunoprecipitation (*IP*) step are shown in the *left panel* (before IP). *B,* co-immunoprecipitation was carried out as described in *A*. In this set of experiments, we also included samples obtained from COS-7 cells transfected with the indicated DREADDs or β-arrestin-1 (*β-αrr1*) alone. *Arrows* indicate immunoreactive species corresponding in size to the M3D and M3D-arr DREADDs. Note that the M3D-Gq designer receptor could not be immunoprecipitated with β-arrestin-1 under the chosen experimental conditions (*A* and *B*). The blots shown are representative of three independent experiments.

Two to 3 weeks after AAV injections, we carried out Western blotting experiments to confirm that all DREADDs were selectively expressed in the liver. Fig. 6 clearly shows that all DREADDs gave a strong immunoreactive signal in the liver but not in any of the other tissues investigated. We also carried out [^{3}H]NMS binding assays using membranes prepared from DREADD-expressing primary mouse hepatocytes. These studies showed all DREADDs, including M3D-Gq, were expressed at high levels in mouse hepatocytes ranging from ~0.7 to 1 pmol/mg protein (Table 3).

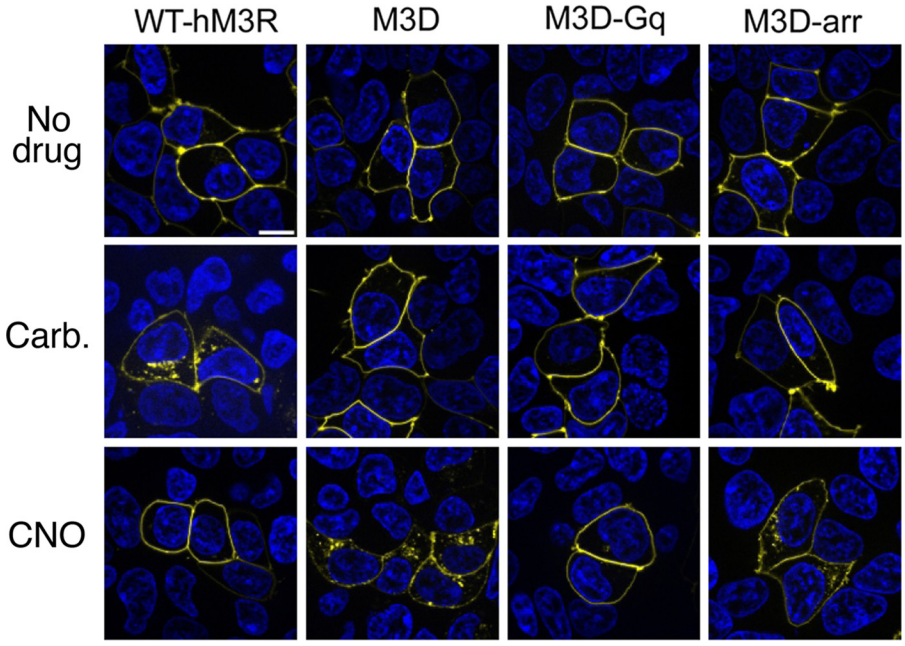


FIGURE 5. **DREADD internalization assays.** HEK293 cells were transfected with the WT human M3R (*WT-hM3R*) and the indicated DREADDs fused to EYFP (*yellow*) at their C termini. Live-cell imaging studies were performed 24 h after transfection using a Zeiss Axio Observer microscope. Nuclei were stained with Hoechst 33324 (*blue*). To study receptor internalization, cells were incubated for 45 min with carbachol (*Carb.*) or CNO (100 μM each). Images were acquired before (*no drug*) and after agonist treatment. In contrast to all other receptor/DREADD constructs, the M3D-Gq designer receptor failed to undergo agonist (CNO)-dependent internalization. *Scale bar,* 10 μM.

CNO Stimulation of M3D-Gq-expressing Primary Mouse Hepatocytes Leads to Robust Calcium Responses—To examine whether M3D-Gq retained its ability to activate G_q-type G proteins in hepatocytes, we isolated primary hepatocytes from mice injected with the AAV-TBG-M3D-Gq virus. In parallel, we also prepared hepatocytes from mice treated with the AAV-TBG-M3D and AAV-TBG-M3D-arr viruses. We then used FLIPR to monitor CNO-mediated increases in $[Ca^{2+}]_i$ in DREADD-expressing hepatocytes. CNO treatment of M3D-Gq-expressing hepatocytes led to pronounced elevations in $[Ca^{2+}]_i$, in the same fashion as observed with M3D-expressing hepatocytes (Table 3; Fig. 7). In contrast, CNO had no significant effect on $[Ca^{2+}]_i$ in M3D-arr-expressing hepatocytes (Fig. 7). These data indicated that M3D-Gq, similar to M3D, can efficiently couple to $G_{q/11}$ in endogenous cells (hepatocytes).

Activation of DREADDs Expressed in Hepatocytes In Vivo—It is well known that endogenous GPCRs can regulate hepatic glucose fluxes, resulting in changes in blood glucose levels (41). For example, treatment of mice with glucagon leads to pronounced hyperglycemia, caused by the activation of G_s-coupled glucagon receptors that are abundantly expressed by hepatocytes and strongly stimulate hepatic glucose production (42, 43). We recently demonstrated that CNO treatment of transgenic mice expressing the M3D DREADD selectively in hepatocytes leads to robust increases in blood glucose levels, due to enhanced hepatic gluconeogenesis and glycogen breakdown (44). To examine whether this effect is mediated exclusively by the activation of hepatocyte $G_{q/11}$ or whether β-arrestin-dependent signaling pathways also contribute to this response, we carried out the following *in vivo* study. Mice that had been injected with the different DREADD AAVs (AAV-TBG-M3D-Gq, AAV-TBG-M3D, or AAV-TBG-M3D-arr) received a single injection of CNO (10 mg/kg, intraperitoneal), followed by the monitoring of blood glucose levels over the next 90 min. Strikingly, CNO treatment of mice that had been injected with the M3D-Gq virus led to robust increases in blood glucose levels (Fig. 8). The magnitude and time course of this response was very similar to that observed with mice that had been treated with the M3D virus (Fig. 8). In striking contrast, CNO treatment of mice that had been injected with the M3D-arr virus did not cause significant elevations in blood glucose levels, as compared with mice that had received the control eGFP virus (Fig. 8). Taken together, these data strongly suggest that β-arrestin-dependent signaling pathways do not play a significant role in M3D-induced hyperglycemia.

CNO Treatment of M3D-Gq-expressing Primary Hepatocytes Stimulates Glucose Release—The most likely explanation for the hyperglycemic effects observed after CNO treatment of mice injected with the M3D-Gq virus is that activation of hepatic M3D-Gq receptors promotes hepatic glucose production (HGP). To test this hypothesis in a more direct fashion, we studied HGP using primary hepatocytes prepared from mice that had received the M3D-Gq virus. CNO (10 μM) or glucagon (control; 100 nM) treatment of M3D-Gq hepatocytes led to significant increases in HGP (Fig. 9). The magnitude of these effects was similar to that observed with M3D hepatocytes (Fig. 9). The M3D-Gq-mediated increase in HGP could be completely blocked in the presence of the muscarinic antagonist, NMS (100 μM; $n = 3$). CNO treatment of M3D-arr hepatocytes had no significant effect on HGP. These data strongly support the notion that the hyperglycemic effects observed after CNO treatment of mice injected with the M3D-Gq virus are caused by a direct effect on hepatocytes.

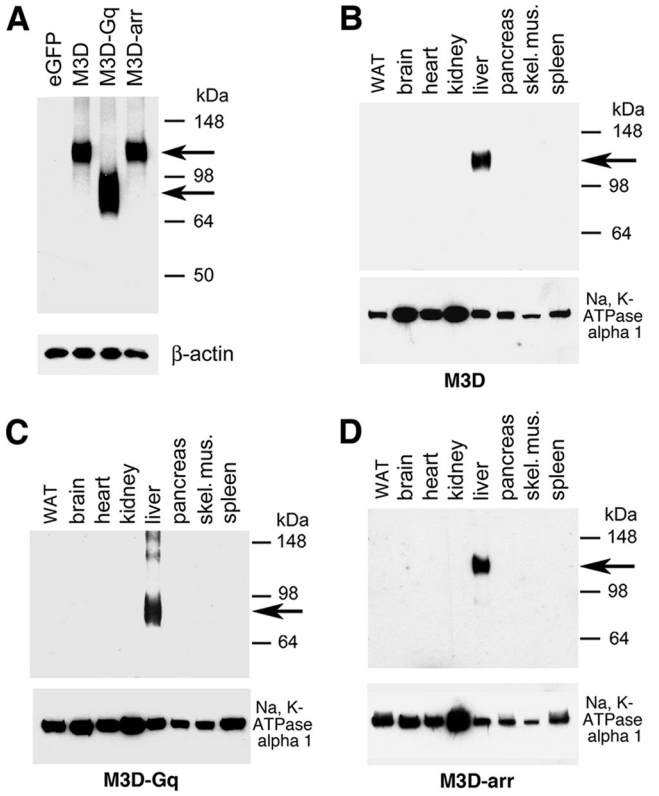


FIGURE 6. **Liver/hepatocyte-specific expression of DREADDs in mice.** WT mice (8-week-old males) were injected i.v. with recombinant AAV-TBG-DREADD viruses coding for the indicated DREADDs. About 2–3 weeks later, the liver-specific expression of the various DREADDs was studied via Western blotting. *A,* immunoblot showing DREADD expression in hepatocytes isolated from AAV-TBG-DREADD-injected mice. Because all DREADDs carried an N-terminal HA tag, DREADD expression was visualized by the use of a monoclonal anti-HA antibody. Note that no immunoreactive band was observed with hepatocytes prepared from mice injected with a control AAV (AAV-TBG-eGFP). *B–D,* selective expression of DREADDs in the liver of AAV-TBG-DREADD-injected mice. Membrane lysates were prepared from the indicated tissues obtained from AAV-TBG-DREADD-injected mice (*B*, M3D; *C*, M3D-Gq; *D*, M3D-arr). Membrane extracts were then subjected to SDS-PAGE under reducing conditions, and DREADD expression was studied via Western blotting using a monoclonal anti-HA antibody. *Arrows* indicate bands corresponding to the different DREADDs. The blots shown are representative of three independent experiments. *WAT,* white adipose tissue; *skel. musc.,* skeletal muscle.

TABLE 3

Ligand binding and functional properties of DREADDs expressed in primary mouse hepatocytes

Experiments were carried out with primary hepatocytes prepared from WT mice that had been injected with AAVs coding for eGFP (control) or the indicated DREADDs. [^{3}H]NMS saturation binding and FLIPR experiments were performed as described under "Experimental Procedures." Binding data are presented as means ± S.E. of 3–5 independent experiments, each carried out in duplicate. CNO-induced increases in $[Ca^{2+}]_i$ were determined using FLIPR. $[Ca^{2+}]_i$ data are given as means ± S.E. of three or four independent experiments, each performed in quadruplicate.

Construct	[^{3}H]NMS binding B_{max}	CNO-induced Ca^{2+} mobilization	
		EC_{50}	E_{max}
	pmol/mg protein	*nM*	*-fold over basal*
eGFP	NB[a]	NR[b]	
M3D	0.67 ± 0.19	85 ± 14	7.3 ± 2.3
M3D-Gq	1.05 ± 0.34	215 ± 58	9.8 ± 1.8
M3D-arr	0.88 ± 0.06	NR	

[a] NB means no detectable specific radioligand binding activity.
[b] NR means no significant response up to 50 μM CNO.

Effect of $G\alpha_{q/11}$ Knockdown on M3D-Gq-mediated Hepatic Glucose Output—To demonstrate the involvement of G_q-type G proteins in M3D-Gq-mediated hepatic glucose release, we

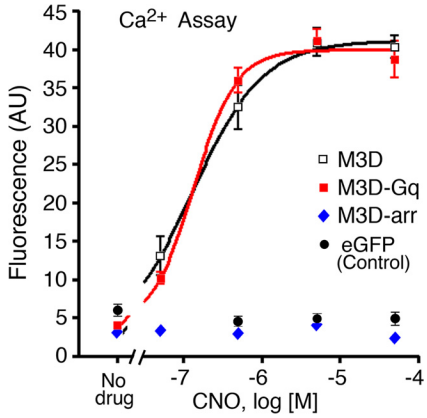


FIGURE 7. **CNO treatment of M3D-Gq-expressing primary hepatocytes results in a pronounced increase in $[Ca^{2+}]_i$.** FLIPR assays were carried out with primary hepatocytes expressing eGFP (*control*) or the indicated DREADDs. CNO-induced increases in $[Ca^{2+}]_i$ were determined as described under "Experimental Procedures." The curves shown are from a representative experiment, carried out in quadruplicate. Two additional experiments gave similar results. Mean CNO EC_{50} and E_{max} values are given in Table 3.

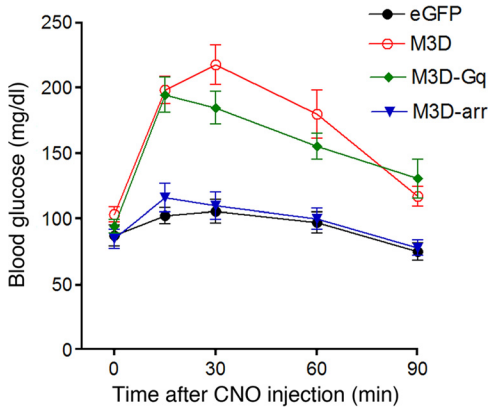


FIGURE 8. **Functional expression of M3D-Gq in mouse hepatocytes *in vivo*.** WT mice (8-week-old males) were injected i.v. with recombinant AAV-TBG-DREADD viruses coding for the indicated DREADDs or with a control virus (AAV-TBG-eGFP) encoding eGFP. Two weeks later, mice were fasted overnight and then injected with CNO (10 mg/kg intraperitoneally). The resulting changes in blood glucose levels were monitored over 90 min. CNO-mediated activation of the M3D and M3D-Gq designer receptors led to robust increases in blood glucose levels. In contrast, CNO treatment of M3D-arr-expressing mice, similar to eGFP control mice, had little or no effect on blood glucose levels. Data are given as means ± S.E. (n = 7–14 mice per group).

treated primary mouse hepatocytes expressing the M3D-Gq construct with either scrambled control siRNA or $G\alpha_{q/11}$ siRNA. As expected, we found that the CNO-induced increase in glucose production in M3D-Gq-expressing hepatocytes was significantly reduced after knockdown of $G\alpha_{q/11}$ expression (Fig. 10*A*). $G\alpha_{q/11}$ siRNA treatment did not completely abolish the CNO/M3D-Gq-mediated glucose response, most likely due to the residual $G\alpha_q$ expression (Fig. 10*B*).

M3D-arr Construct Undergoes CNO-induced Internalization in Mouse Hepatocytes—To confirm that the M3D-arr construct remained functional when expressed in mouse hepatocytes, we incubated M3D-arr expressing hepatocytes for 1 h with or without CNO (10 μM). Subsequently, we determined cell surface M3D-arr expression levels by incubation of intact cells with [^{3}H]NMS (10 nM), a membrane-impermeable muscarinic radioligand. These experiments confirmed that the M3D-arr

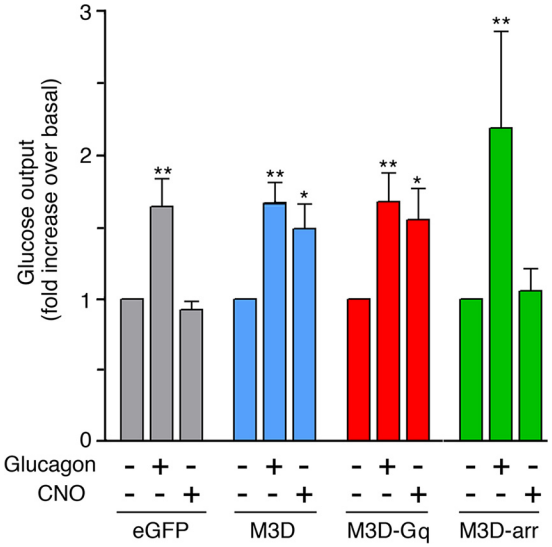


FIGURE 9. **DREADD-mediated increases in HGP studied with isolated hepatocytes.** Primary hepatocytes were isolated from WT mice (8-week-old males) that had been injected i.v. with recombinant AAV-TBG-DREADD viruses coding for the indicated DREADDs or with a control virus (AAV-TBG-eGFP) encoding eGFP. Hepatocytes were first maintained in glucose-free medium for 16 h and then incubated with CNO (10 μM) or glucagon (100 nM; positive control) for 4 h at 37 °C. After this time, glucose concentrations were determined in the culture medium. Basal glucose release did not differ significantly among eGFP- and DREADD-expressing hepatocytes (data range: 0.03–0.10 μg of glucose/μg of protein). Data are given as means ± S.E. of three independent experiments.*, $p < 0.05$; **, $p < 0.01$, as compared with non-treated cells.

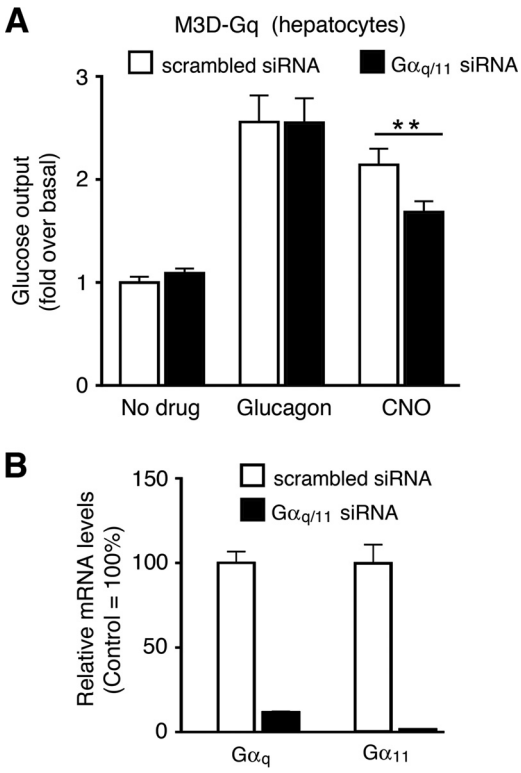


FIGURE 10. **CNO-induced glucose output in M3D-Gq-expressing hepatocytes is greatly reduced after $G\alpha_{q/11}$ knockdown.** Primary mouse hepatocytes expressing the M3D-Gq construct were treated with either scrambled control siRNA or $G\alpha_{q/11}$ siRNA. *A*, glucose release studies. To stimulate glucose production, hepatocytes were incubated with CNO (10 μM) or glucagon (100 nM; positive control) for 4 h at 37 °C. After this step, glucose concentrations were determined in the culture medium. *B*, effective knockdown of $G\alpha_{q/11}$ expression after treatment of M3D-Gq-expressing mouse hepatocytes with $G\alpha_{q/11}$ siRNA. $G\alpha_{q/11}$ transcript levels were determined by quantitative RT-PCR using standard techniques. Data are given as means ± S.E. of three independent experiments.**, $p < 0.01$, as compared with the control group.

construct retained the ability to undergo agonist-induced internalization ([^{3}H]NMS-binding sites in fmol/mg protein: no CNO treatment, 1258 ± 64; after CNO treatment, 1053 ± 20; $n = 3$; $p < 0.001$).

Discussion

GPCRs are named after their ability to interact with and activate heterotrimeric G proteins. Ligand-activated GPCRs also bind to members of the arrestin family (β-arrestin-1 and -2), which disrupt receptor/G protein coupling and promote GPCR internalization via well known processes (7, 40). Accumulating evidence indicates that β-arrestin-1 and -2, following their recruitment to activated GPCRs, can also act as signaling molecules in their own right. It has become clear during the past 10–15 years that numerous signaling pathways and cellular processes can be activated or inhibited by β-arrestin-1 and/or -2 in a G protein-independent fashion (9–12, 15, 40). The overall signaling outcome caused by activation of a specific GPCR in a particular cell type is considered a combination of both G protein- and β-arrestin (G protein-independent)-mediated signaling events (9–13). In this study, we focused on the development of a novel, G protein-biased DREADD as a tool to deconvolute this signaling complexity. As discussed below, a better understanding of the relative contributions of these two branches of GPCR signaling to specific GPCR-mediated physiological responses is of considerable potential clinical importance (9–11, 14–17).

Here, we describe the generation and pharmacological properties of a novel $G_{q/11}$-biased DREADD (referred to as M3D-Gq) that shows signal properties opposite to those of M3D-arr, a β-arrestin-biased DREADD (18). CNO treatment of M3D-Gq leads to the efficient activation of G_q-type G proteins but does not promote β-arrestin recruitment (Figs. 2–5). To demonstrate that the M3D-Gq designer receptor was also functional *in vivo*, we selectively expressed M3D-Gq in hepatocytes of WT mice (Fig. 6). We found that CNO treatment of the M3D-Gq-expressing mice resulted in pronounced hyperglycemic responses (Fig. 8), most likely due to an increase in HGP, as suggested by studies with isolated hepatocytes (Fig. 9). In contrast, CNO treatment of mice selectively expressing the M3D-arr DREADD in hepatocytes had no significant effect on blood glucose levels (Fig. 8), and addition of CNO to M3D-arr-expressing hepatocytes had no effect on HGP (Fig. 9). These data indicate that the ability of G_q-coupled receptors to promote HGP is exclusively dependent on $G_{q/11}$-mediated signaling and does not require β-arrestin-activated signaling pathways. Hepatocytes express several endogenous G_q-coupled receptors, including α_1-adrenergic and V_1 vasopressin receptors (41). As proposed previously (41), the ability of this class of GPCRs to stimulate glucose release from the liver is most likely due to $G_{q/11}$-mediated increases in $[Ca^{2+}]_i$, which in turn lead to the activation of enzymes that enhance HGP. Interestingly, we recently demonstrated that blockade of hepatic V_1 receptors is able to significantly ameliorate the deficits in glucose homeostasis observed in a mouse model of obesity (*ob/ob* mice (44)). Agents that can block $G_{q/11}$-mediated signaling in

hepatocytes may therefore prove beneficial clinically for reducing HGP and hyperglycemia in type 2 diabetes, a disease that is characterized by unphysiologically elevated HGP (45, 46).

It is well known that β-arrestin-mediated signaling regulates long term processes involving various signaling cascades that lead to changes in gene expression (9–13). Thus, we cannot exclude the possibility that β-arrestins modulate hepatic glucose fluxes under different experimental conditions where HGP is monitored for days or weeks.

A previous study has shown that acute intraperitoneal treatment of mice with CNO does not lead to detectable levels of clozapine in the plasma (5). For this reason, it is unlikely that the findings described in this study were affected by back-transformation of CNO to clozapine. However, it should be noted that the metabolic transformation of CNO after chronic administration has not been studied systematically in mice.

Although the viral delivery approach that we employed in this study resulted in relatively high DREADD expression levels, the observed functional responses were mediated by endogenous G proteins and other signaling proteins. Also, the measured DREADD expression levels are not out of the physiological range because several GPCRs, including different muscarinic receptor subtypes (47), are expressed at comparable levels in other tissues.

The generation and analysis of G protein- and β-arrestin-biased DREADDs is highly relevant to recent advances in the development of G protein- and β-arrestin-biased agonists (11, 14, 15, 17, 48). Various lines of evidence suggest that the potential clinical use of functionally biased agonists may be associated with increased therapeutic efficacy and reduced side effects, at least in certain clinical conditions (11, 14, 17, 48). For example, several studies suggest that G protein-biased μ-opioid receptor agonists may be able to relieve pain without causing the characteristic side effects (tolerance, addiction, etc.) associated with the use of morphine and other non-biased μ-receptor agonists (11). Similarly, G protein-biased κ-opioid receptor agonists may prove clinically useful as novel analgesic agents endowed with fewer side effects such as sedation, motor incoordination, and anhedonia (49).

The outcome of physiological studies using G protein- and β-arrestin-biased DREADDs should prove particularly useful in guiding the search for novel biased ligands with therapeutic potential. The great advantage of DREADD technology is that it allows the activation of distinct signaling pathways in a particular cell type *in vivo*. As a consequence, such DREADD studies offer direct insights into the cellular basis of an observed physiological or behavioral response. In contrast, the situation is considerably more complex in the case of G protein- and β-arrestin-biased ligands, which after their systemic administration usually act on target receptors expressed in multiple tissues or cell types. Thus, DREADD technology clearly complements ongoing efforts in the "biased GPCR ligand" field, offering the opportunity of identifying novel targets for the development of G protein- and β-arrestin-biased ligands.

Author Contributions—J. H., M. S., L. E. G., L. W., L. Z., M. R., and J. M. collected and analyzed experimental data. A. I. provided novel experimental tools. J. H., A. G. B.-S., V. V. G., and J. W. designed experiments and wrote the paper. All authors examined the results and approved the final version of the manuscript.

Acknowledgments—We thank Kelly Hu and Theresa Bödefeld (NIDDK, National Institutes of Health) for their experimental contributions to this work.

References

1. Rogan, S. C., and Roth, B. L. (2011) Remote control of neuronal signaling. *Pharmacol. Rev.* **63,** 291–315
2. Wess, J., Nakajima, K., and Jain, S. (2013) Novel designer receptors to probe GPCR signaling and physiology. *Trends Pharmacol. Sci.* **34,** 385–392
3. Urban, D. J., and Roth, B. L. (2015) DREADDs (designer receptors exclusively activated by designer drugs): chemogenetic tools with therapeutic utility. *Annu. Rev. Pharmacol. Toxicol.* **55,** 399–417
4. Armbruster, B. N., Li, X., Pausch, M. H., Herlitze, S., and Roth, B. L. (2007) Evolving the lock to fit the key to create a family of G protein-coupled receptors potently activated by an inert ligand. *Proc. Natl. Acad. Sci. U.S.A.* **104,** 5163–5168
5. Guettier, J. M., Gautam, D., Scarselli, M., Ruiz de Azua, I., Li, J. H., Rosemond, E., Ma, X., Gonzalez, F. J., Armbruster, B. N., Lu, H., Roth, B. L., and Wess, J. (2009) A chemical-genetic approach to study G protein regulation of beta cell function *in vivo*. *Proc. Natl. Acad. Sci. U.S.A.* **106,** 19197–19202
6. Regard, J. B., Sato, I. T., and Coughlin, S. R. (2008) Anatomical profiling of G protein-coupled receptor expression. *Cell* **135,** 561–571
7. Pierce, K. L., Premont, R. T., and Lefkowitz, R. J. (2002) Seven-transmembrane receptors. *Nat. Rev. Mol. Cell Biol.* **3,** 639–650
8. Gainetdinov, R. R., Premont, R. T., Bohn, L. M., Lefkowitz, R. J., and Caron, M. G. (2004) Desensitization of G protein-coupled receptors and neuronal functions. *Annu. Rev. Neurosci.* **27,** 107–144
9. Shukla, A. K., Xiao, K., and Lefkowitz, R. J. (2011) Emerging paradigms of β-arrestin-dependent seven transmembrane receptor signaling. *Trends Biochem. Sci.* **36,** 457–469
10. Luttrell, L. M., and Gesty-Palmer, D. (2010) Beyond desensitization: physiological relevance of arrestin-dependent signaling. *Pharmacol. Rev.* **62,** 305–330
11. Luttrell, L. M., Maudsley, S., and Bohn, L. M. (2015) Fulfilling the promise of "biased" G protein-coupled receptor agonism. *Mol. Pharmacol.* **88,** 579–588
12. Gurevich, V. V., and Gurevich, E. V. (2014) Overview of different mechanisms of arrestin-mediated signaling. *Curr. Protoc. Pharmacol.* **67,** Unit 2.10, 10.1002/0471141755.ph0210s67
13. Beaulieu, J. M., Gainetdinov, R. R., and Caron, M. G. (2009) Akt/GSK3 signaling in the action of psychotropic drugs. *Annu. Rev. Pharmacol. Toxicol.* **49,** 327–347
14. Shonberg, J., Lopez, L., Scammells, P. J., Christopoulos, A., Capuano, B., and Lane, J. R. (2014) Biased agonism at G protein-coupled receptors: the promise and the challenges–a medicinal chemistry perspective. *Med. Res. Rev.* **34,** 1286–1330
15. Zhou, L., and Bohn, L. M. (2014) Functional selectivity of GPCR signaling in animals. *Curr. Opin. Cell Biol.* **27,** 102–108
16. Whalen, E. J., Rajagopal, S., and Lefkowitz, R. J. (2011) Therapeutic potential of β-arrestin- and G protein-biased agonists. *Trends Mol. Med.* **17,** 126–139
17. Kenakin, T., and Christopoulos, A. (2013) Signalling bias in new drug discovery: detection, quantification and therapeutic impact. *Nat. Rev. Drug Discov.* **12,** 205–216
18. Nakajima, K., and Wess, J. (2012) Design and functional characterization of a novel, arrestin-biased designer G protein-coupled receptor. *Mol. Pharmacol.* **82,** 575–582
19. Alvarez-Curto, E., Prihandoko, R., Tautermann, C. S., Zwier, J. M., Pediani, J. D., Lohse, M. J., Hoffmann, C., Tobin, A. B., and Milligan, G. (2011) Developing chemical genetic approaches to explore G protein-coupled receptor function: validation of the use of a receptor activated solely by synthetic ligand (RASSL). *Mol. Pharmacol.* **80,** 1033–1046
20. Scarselli, M., Li, B., Kim, S. K., and Wess, J. (2007) Multiple residues in the second extracellular loop are critical for M3 muscarinic acetylcholine receptor activation. *J. Biol. Chem.* **282,** 7385–7396

21. Hu, J., Wang, Y., Zhang, X., Lloyd, J. R., Li, J. H., Karpiak, J., Costanzi, S., and Wess, J. (2010) Structural basis of G protein-coupled receptor-G protein interactions. *Nat. Chem. Biol.* **6,** 541–548
22. Gimenez, L. E., Kook, S., Vishnivetskiy, S. A., Ahmed, M. R., Gurevich, E. V., and Gurevich, V. V. (2012) Role of receptor-attached phosphates in binding of visual and non-visual arrestins to G protein-coupled receptors. *J. Biol. Chem.* **287,** 9028–9040
23. Gimenez, L. E., Vishnivetskiy, S. A., Baameur, F., and Gurevich, V. V. (2012) Manipulation of very few receptor discriminator residues greatly enhances receptor specificity of non-visual arrestins. *J. Biol. Chem.* **287,** 29495–29505
24. Vishnivetskiy, S. A., Gimenez, L. E., Francis, D. J., Hanson, S. M., Hubbell, W. L., Klug, C. S., and Gurevich, V. V. (2011) Few residues within an extensive binding interface drive receptor interaction and determine the specificity of arrestin proteins. *J. Biol. Chem.* **286,** 24288–24299
25. Wan, M., Leavens, K. F., Saleh, D., Easton, R. M., Guertin, D. A., Peterson, T. R., Kaestner, K. H., Sabatini, D. M., and Birnbaum, M. J. (2011) Postprandial hepatic lipid metabolism requires signaling through Akt2 independent of the transcription factors FoxA2, FoxO1, and SREBP1c. *Cell Metab.* **14,** 516–527
26. Li, P., Ruan, X., Yang, L., Kiesewetter, K., Zhao, Y., Luo, H., Chen, Y., Gucek, M., Zhu, J., and Cao, H. (2015) A liver-enriched long non-coding RNA, lncLSTR, regulates systemic lipid metabolism in mice. *Cell Metab.* **21,** 455–467
27. Rossi, M., Ruiz de Azua, I., Barella, L. F., Sakamoto, W., Zhu, L., Cui, Y., Lu, H., Rebholz, H., Matschinsky, F. M., Doliba, N. M., Butcher, A. J., Tobin, A. B., and Wess, J. (2015) CK2 acts as a potent negative regulator of receptor-mediated insulin release *in vitro* and *in vivo*. *Proc. Natl. Acad. Sci. U.S.A.* **112,** E6818–E6824
28. Budd, D. C., McDonald, J. E., and Tobin, A. B. (2000) Phosphorylation and regulation of a $G_{q/11}$-coupled receptor by casein kinase 1α. *J. Biol. Chem.* **275,** 19667–19675
29. Torrecilla, I., Spragg, E. J., Poulin, B., McWilliams, P. J., Mistry, S. C., Blaukat, A., and Tobin, A. B. (2007) Phosphorylation and regulation of a G protein-coupled receptor by protein kinase CK2. *J. Cell Biol.* **177,** 127–137
30. Kong, K. C., Butcher, A. J., McWilliams, P., Jones, D., Wess, J., Hamdan, F. F., Werry, T., Rosethorne, E. M., Charlton, S. J., Munson, S. E., Cragg, H. A., Smart, A. D., and Tobin, A. B. (2010) M3-muscarinic receptor promotes insulin release via receptor phosphorylation/arrestin-dependent activation of protein kinase D1. *Proc. Natl. Acad. Sci. U.S.A.* **107,** 21181–21186
31. Schöneberg, T., Liu, J., and Wess, J. (1995) Plasma membrane localization and functional rescue of truncated forms of a G protein-coupled receptor. *J. Biol. Chem.* **270,** 18000–18006
32. Maggio, R., Barbier, P., Fornai, F., and Corsini, G. U. (1996) Functional role of the third cytoplasmic loop in muscarinic receptor dimerization. *J. Biol. Chem.* **271,** 31055–31060
33. Kirchberg, K., Kim, T. Y., Möller, M., Skegro, D., Dasara Raju, G., Granzin, J., Büldt, G., Schlesinger, R., and Alexiev, U. (2011) Conformational dynamics of helix 8 in the GPCR rhodopsin controls arrestin activation in the desensitization process. *Proc. Natl. Acad. Sci. U.S.A.* **108,** 18690–18695
34. Rahmeh, R., Damian, M., Cottet, M., Orcel, H., Mendre, C., Durroux, T., Sharma, K. S., Durand, G., Pucci, B., Trinquet, E., Zwier, J. M., Deupi, X., Bron, P., Banères, J. L., Mouillac, B., and Granier, S. (2012) Structural insights into biased G protein-coupled receptor signaling revealed by fluorescence spectroscopy. *Proc. Natl. Acad. Sci. U.S.A.* **109,** 6733–6738
35. Liu, J. J., Horst, R., Katritch, V., Stevens, R. C., and Wüthrich, K. (2012) Biased signaling pathways in β2-adrenergic receptor characterized by ^{19}F-NMR. *Science* **335,** 1106–1110
36. Wacker, D., Wang, C., Katritch, V., Han, G. W., Huang, X. P., Vardy, E., McCorvy, J. D., Jiang, Y., Chu, M., Siu, F. Y., Liu, W., Xu, H. E., Cherezov, V., Roth, B. L., and Stevens, R. C. (2013) Structural features for functional selectivity at serotonin receptors. *Science* **340,** 615–619
37. Kang, Y., Zhou, X. E., Gao, X., He, Y., Liu, W., Ishchenko, A., Barty, A., White, T. A., Yefanov, O., Han, G. W., Xu, Q., de Waal, P. W., Ke, J., Tan, M. H., Zhang, C., *et al.* (2015) Crystal structure of rhodopsin bound to arrestin by femtosecond x-ray laser. *Nature* **523,** 561–567
38. Shukla, A. K., Westfield, G. H., Xiao, K., Reis, R. I., Huang, L. Y., Tripathi-Shukla, P., Qian, J., Li, S., Blanc, A., Oleskie, A. N., Dosey, A. M., Su, M., Liang, C. R., Gu, L. L., Shan, J. M., *et al.* (2014) Visualization of arrestin recruitment by a G-protein-coupled receptor. *Nature* **512,** 218–222
39. Schrage, R., Schmitz, A. L., Gaffal, E., Annala, S., Kehraus, S., Wenzel, D., Büllesbach, K. M., Bald, T., Inoue, A., Shinjo, Y., Galandrin, S., Shridhar, N., Hesse, M., Grundmann, M., Merten, N., *et al.* (2015) The experimental power of FR900359 to study Gq-regulated biological processes. *Nat. Commun.* **6,** 10156
40. Pierce, K. L., and Lefkowitz, R. J. (2001) Classical and new roles of β-arrestins in the regulation of G-protein-coupled receptors. *Nat. Rev. Neurosci.* **2,** 727–733
41. Exton, J. H. (1987) Mechanisms of hormonal regulation of hepatic glucose metabolism. *Diabetes Metab. Rev.* **3,** 163–183
42. Jiang, G., and Zhang, B. B. (2003) Glucagon and regulation of glucose metabolism. *Am. J. Physiol. Endocrinol. Metab.* **284,** E671–E678
43. Estall, J. L., and Drucker, D. J. (2006) Glucagon and glucagon-like peptide receptors as drug targets. *Curr. Pharm. Des.* **12,** 1731–1750
44. Li, J. H., Jain, S., McMillin, S. M., Cui, Y., Gautam, D., Sakamoto, W., Lu, H., Jou, W., McGuinness, O. P., Gavrilova, O., and Wess, J. (2013) A novel experimental strategy to assess the metabolic effects of selective activation of a G(q)-coupled receptor in hepatocytes *in vivo*. *Endocrinology* **154,** 3539–3551
45. Lin, H. V., and Accili, D. (2011) Hormonal regulation of hepatic glucose production in health and disease. *Cell Metab.* **14,** 9–19
46. Tahrani, A. A., Bailey, C. J., Del Prato, S., and Barnett, A. H. (2011) Management of type 2 diabetes: new and future developments in treatment. *Lancet* **378,** 182–197
47. Oki, T., Takagi, Y., Inagaki, S., Taketo, M. M., Manabe, T., Matsui, M., and Yamada, S. (2005) Quantitative analysis of binding parameters of [3H]N-methylscopolamine in central nervous system of muscarinic acetylcholine receptor knockout mice. *Brain Res. Mol. Brain Res.* **133,** 6–11
48. Wisler, J. W., Xiao, K., Thomsen, A. R., and Lefkowitz, R. J. (2014) Recent developments in biased agonism. *Curr. Opin. Cell Biol.* **27,** 18–24
49. White, K. L., Robinson, J. E., Zhu, H., DiBerto, J. F., Polepally, P. R., Zjawiony, J. K., Nichols, D. E., Malanga, C. J., and Roth, B. L. (2015) The G protein-biased κ-opioid receptor agonist RB-64 is analgesic with a unique spectrum of activities *in vivo*. *J. Pharmacol. Exp. Ther.* **352,** 98–109
50. McMillin, S. M., Heusel, M., Liu, T., Costanzi, S., and Wess, J. (2011) Structural basis of M3 muscarinic receptor dimer/oligomer formation. *J. Biol. Chem.* **286,** 28584–28598